OPEN ACCESS

ARTICLE

Global lake carbon burial from endorheic zones since the Last Glacial Maximum and the future projection

Yu Li,[1,*] Xinzhong Zhang,[2] Zhansen Zhang,[1] Mingjun Gao,[1] and Yaxin Xue[1]

*Correspondence: liyu@lzu.edu.cn (Y. L)

Received: October 3, 2024; Accepted: March 18, 2025; Published Online: March 20, 2025; https://doi.org/10.59717/j.xinn-geo.2025.100132

GRAPHICAL ABSTRACT

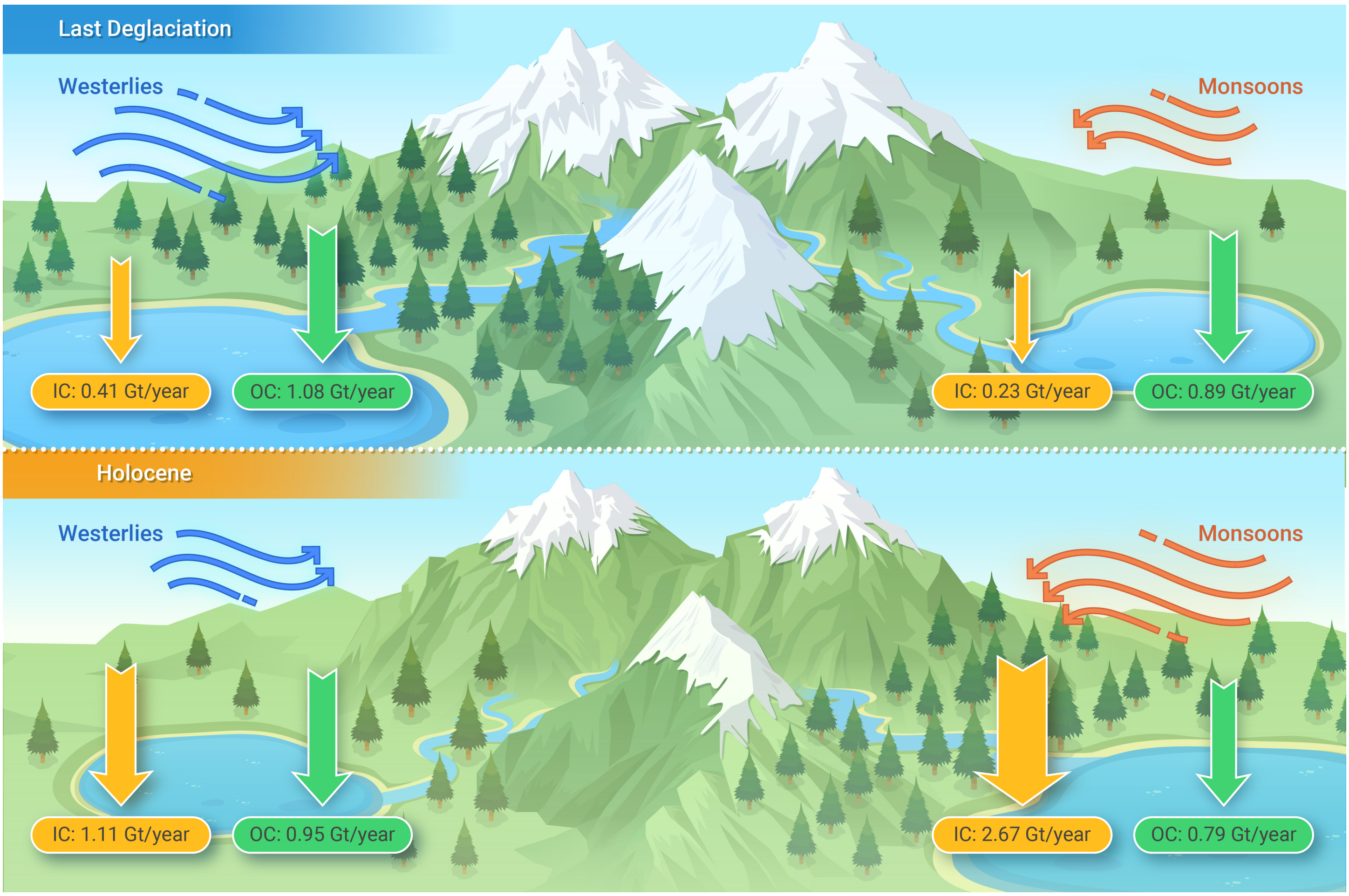

PUBLIC SUMMARY

- Global closed-basin lakes buried twice as much inorganic carbon as organic carbon since the LGM.
- Total carbon burial equals ~10% of dryland soil carbon, highlighting its global carbon cycle role.
- Lake carbon burial rose since the LGM, driven by area fluctuations linked to westerlies and monsoons.
- Projected drying may reduce lake carbon burial by 5% in global closed basins by 2100.

Global lake carbon burial from endorheic zones since the Last Glacial Maximum and the future projection

Yu Li,[1,*] Xinzhong Zhang,[2] Zhansen Zhang,[1] Mingjun Gao,[1] and Yaxin Xue[1]
[1]Key Laboratory of Western China's Environmental Systems (Ministry of Education), College of Earth and Environmental Sciences, Lanzhou University, Lanzhou 730000, China
[2]School of Geography and Tourism, Luoyang Normal University, Luoyang 471000, China
*Correspondence: liyu@lzu.edu.cn (Y. L)
Received: October 3, 2024; Accepted: March 18, 2025; Published Online: March 20, 2025; https://doi.org/10.59717/j.xinn-geo.2025.100132

Citation: Li Y., Zhang X., Zhang Z., et al. (2025). Global lake carbon burial from endorheic zones since the Last Glacial Maximum and the future projection. *The Innovation Geoscience* **3**:100132.

Lake inorganic carbon burial in global closed basins has been recognized as a significant component of the terrestrial carbon cycle. However, the controlling factors governing its long-term dynamics and its future trajectory remain insufficiently understood. Here, we present a comprehensive dataset encompassing lake inorganic and organic carbon burial records from global closed basins since the Last Glacial Maximum (LGM), along with associated lake-level reconstructions, modern observations and climate model outputs. Through integrated analysis of lake carbon burial records and lake area simulation, our results indicate that inorganic carbon burial in closed-basin lakes since the LGM has been approximately twice that of organic carbon burial. The total carbon burial is estimated to be around 174 Pg, which accounts for roughly one-tenth of the soil carbon pool in global drylands, underscoring its significance in the global carbon cycle. Lake carbon burial rate has shown a continuous increase since the LGM, with interannual variations of lake carbon burial amount closely linked to fluctuations in lake area, which are primarily modulated by westerly winds and monsoon circulation in different closed basins. Under future global warming scenarios, with projected drying trend in global closed basins, the lake carbon burial potential by 2100 is estimated to be approximately 1 Pg, which is about 5% lower compared to scenarios with stable lake area, highlighting the substantial role of lake carbon burial in shaping the future global carbon budget.

INTRODUCTION

The global carbon cycle, which operates through key processes such as photosynthesis, fossil fuel combustion, weathering, and volcanism, plays a fundamental role in maintaining Earth's climate stability and carbon balance.[1,2] Among terrestrial carbon reservoirs, soils represent one of the largest surface carbon pools, with significant implications for mitigating global climate change.[3-5] Soil inorganic carbon, predominantly in the form of carbonates, undergoes a relatively stable and prolonged renewal cycle. A portion of this carbon can be leached into aquatic systems, facilitating carbon exchange between terrestrial and aquatic reservoirs.[6] Notably, dryland soils are estimated to contain approximately 80% of the global soil inorganic carbon pool, with significant inorganic carbon sequestration observed in dryland lakes, particularly those in closed-basin systems.[7,8]

As integral components of the terrestrial hydrosphere, lakes serve as critical interfaces between various Earth system components. Despite covering only about 2% of the global land surface, lakes exhibit significantly higher carbon turnover rates than soils and oceans.[9-13] Over long timescales, sedimentary carbon burial represents the primary mechanism of lacustrine carbon sequestration, influenced by climatic conditions, watershed characteristics, lake properties, and anthropogenic activities. While the importance of lakes as terrestrial carbon sinks has gained increasing recognition, the role of inorganic carbon in lake carbon burial remains understudied.[14-17]

Recent advancements have enhanced our understanding of inorganic

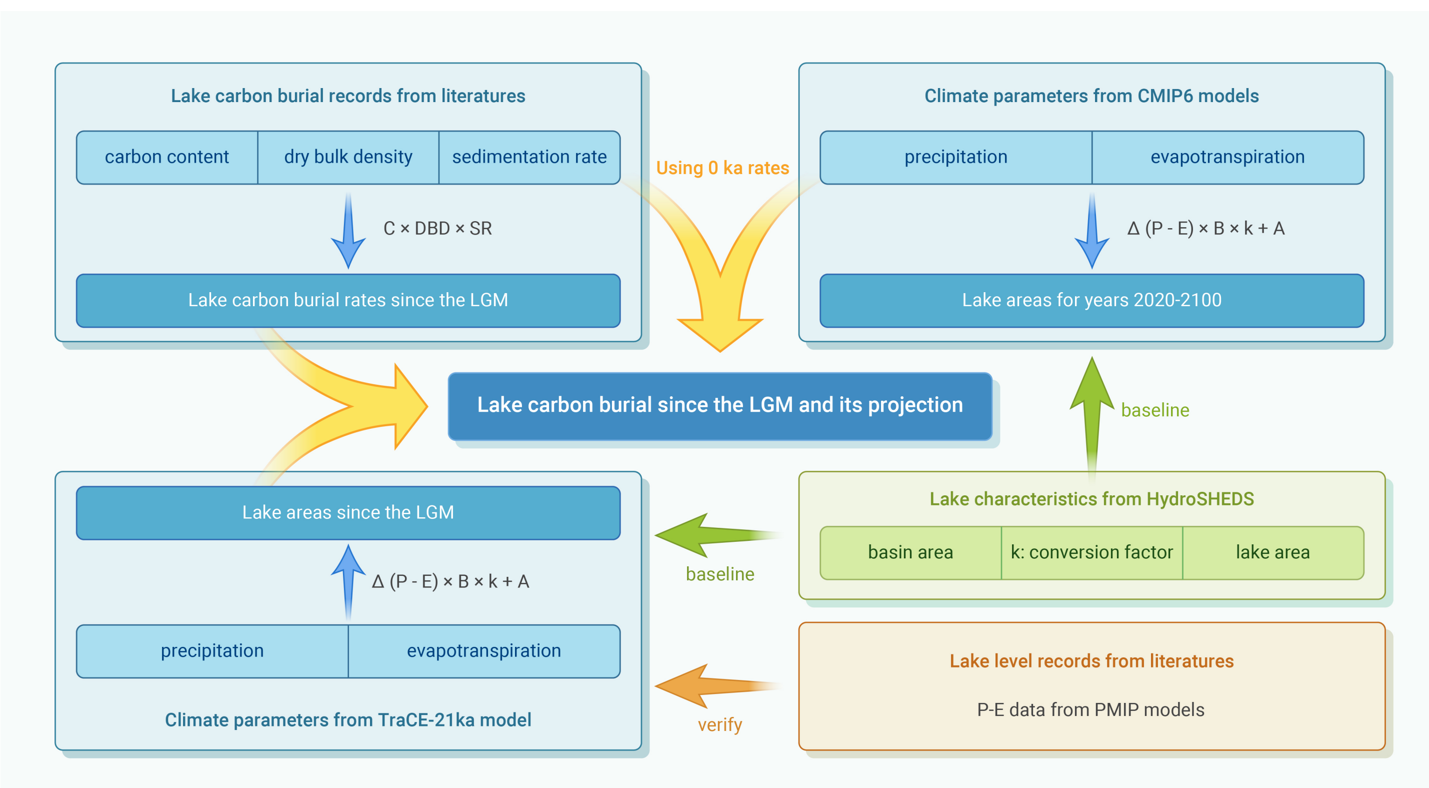

Figure 1. Overall research framework.

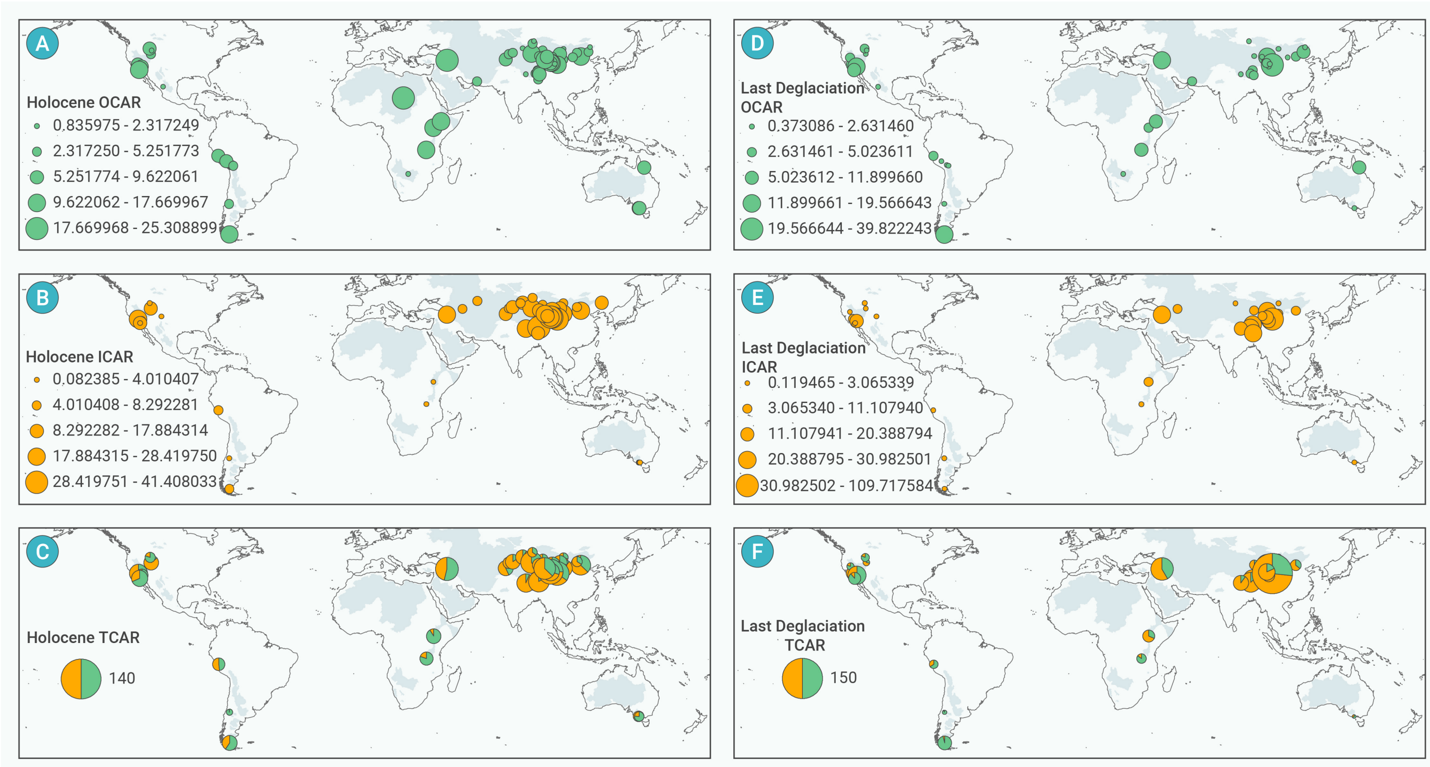

Figure 2. Spatial distributions of mean organic carbon burial rates (OCAR), inorganic carbon burial rates (ICAR), and total carbon burial rates (TCAR) (g/m^2/yr) in global closed-basin lakes during the Holocene (A-C) and Last Deglaciation (D-F).

carbon content and provenance in closed-basin lakes.[7,18] Unlike lake carbon burial in other regions, radiocarbon dating and isotopic analysis suggest that CO_2 absorbed by saline-alkaline soils constitutes the primary source of groundwater dissolved inorganic carbon in closed basins, contributing approximately 50% of the total inorganic carbon flux.[18] This finding indicates that closed-basin lakes act as net sinks of atmospheric CO_2 rather than mere terrestrial carbon transporters. Despite these insights, research on lake carbon burial has predominantly focused on organic carbon,[19] with insufficient attention given to inorganic carbon burial, thereby limiting our comprehensive understanding of lake carbon burial change.

The global endorheic zone, covering approximately one-fifth of the Earth's land surface and primarily located in arid and semi-arid regions, exhibits a relatively isolated and self-contained carbon cycle. This region is characterized by substantial inorganic carbon stocks, often exceeding organic carbon concentrations by several orders of magnitude. The terminal areas of endorheic basins, lacking hydrological connections to oceans, serve as natural integrators of basin-wide sedimentary information, making them ideal for studying lake evolution and carbon burial dynamics. However, in recent decades, water storage in global endorheic lakes has declined at approximately twice the rate observed in exorheic lakes, leading to significant lake shrinkage and, in some cases, complete desiccation.[20] These trends underscore the urgent need to assess carbon burial changes and future sequestration potential in these vulnerable systems.

The pronounced hydroclimatic fluctuations in global closed basins since the LGM,[21] particularly substantial variations in lake areas, provide an opportunity to investigate long-term lake evolution and carbon burial patterns. In this study, we integrate lake sedimentary records, hydroclimatic models, and modern observational data to analyze changes in lake carbon burial and their driving mechanisms in global closed basins since the LGM. We further examine lake evolution patterns during cold and warm climatic periods across different timescales. Finally, by simulating lake area changes and incorporating lake carbon burial data, we estimate the magnitude of carbon burial changes in global closed basins since the LGM and assess future carbon sequestration potential (see Figure 1 for overall research framework). This research contributes to a more comprehensive understanding on the role of lake carbon burial in the global carbon cycle, with implications for achieving global carbon neutrality goals.

MATERIALS AND METHODS

Lake records

The lake record data used in this study include 54 pairs of lake level comparisons between different cold and warm periods and 112 sequences of lake carbon burial records since the LGM (Tables S1-S3 & Figure S1). These data were primarily sourced from peer-reviewed journal articles published over the past three decades. The criterions for lake level record selection are as follows, (1) the records must include direct evidence such as shorelines or continuous lake level reconstructions; (2) Each record must contain at least one pair of lake level comparisons between corresponding cold and warm periods, that is, between the LGM (~21 ka) and mid-Holocene (MH, ~6 ka) or between the Medieval Climate Anomaly (MCA, 950-1250) and Little Ice Age (LIA, 1450-1850);[22] (3) The lake level dating must be reliable, with at least one age control point during the LIA or MCA and two during the LGM or MH. Based on these criteria, 54 sets of comparative data from 38 lakes in global closed basins since the LGM were selected. For selection of lake carbon burial record, (1) the records must include organic carbon content (or proxies such as organic matter content and loss on ignition data) or inorganic carbon content (or proxies such as carbonates content and loss on ignition data); (2) the original sampling resolution must be < 500 years, with continuous records spanning > 6000 years to ensure long-term comparability and avoid overrepresentation of short-term records; (3) Records from lake edges, which are often perturbed and less representative of whole-lake carbon burial, were excluded. All ^{14}C ages were calibrated using the IntCal20 curve via the OxCal online tool, and the piecewise linear interpolation method is used for depth-age model to calculate the sedimentation rate.[23,24]

Calculation of lake carbon burial

Lake carbon burial (T, in t/yr) was calculated using the following formula,

$$T = C \times DBD \times SR \times A \times 100$$

where C is carbon content (%), DBD is dry bulk density (g/cm^3), SR is sedimentation rate (cm/yr), and A is lake area (km^2). For records with other proxy data, carbon content was derived as follows,

$$OC = OrganicMatter \times 0.58$$

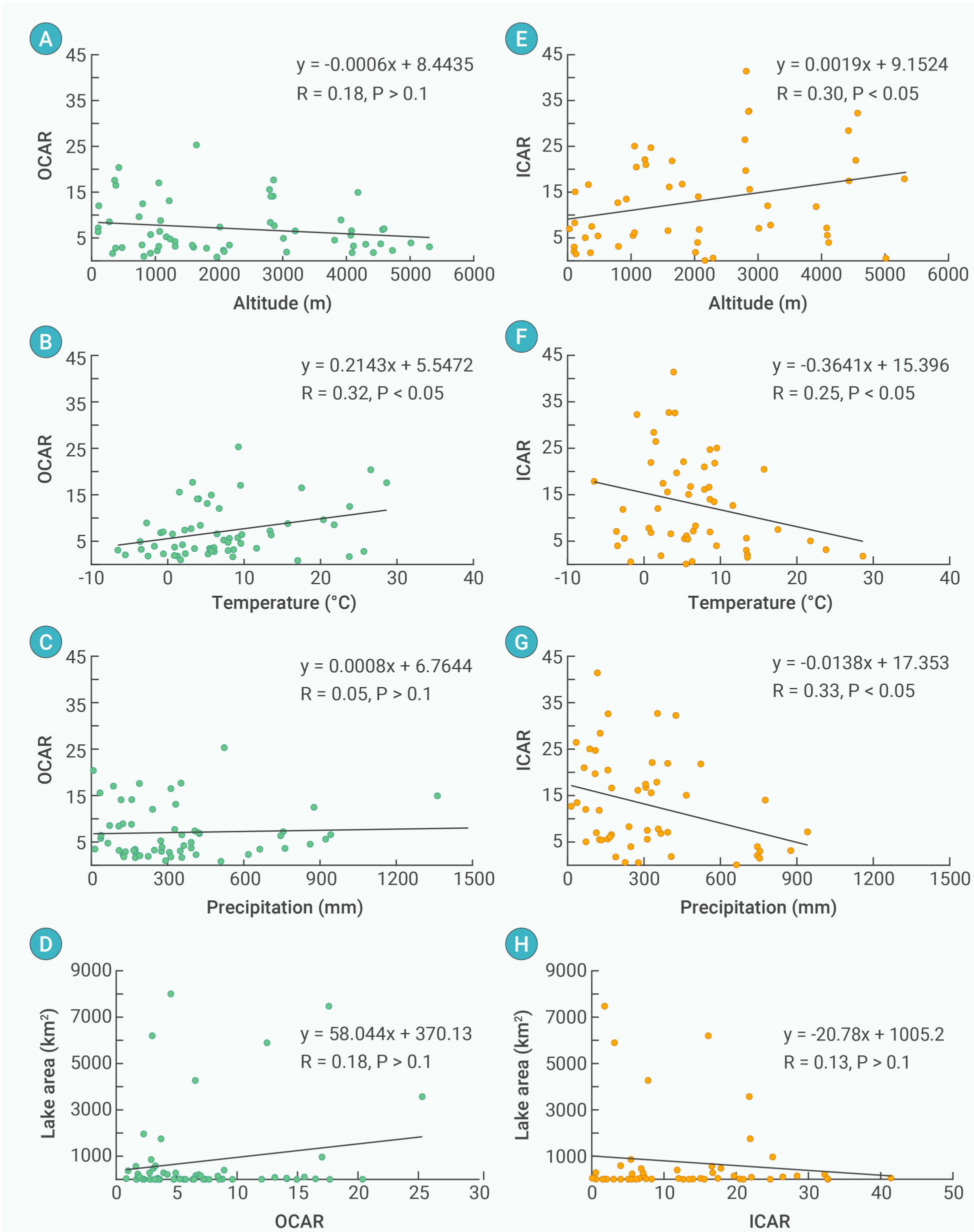

Figure 3. Scatterplots illustrating correlations between lake organic carbon burial rates (OCAR; left column) and inorganic carbon burial rates (ICAR; right column) ($g/m^2/yr$) with altitude, temperature, precipitation, and lake area in global closed basins Black lines represent linear regression fits, with corresponding equations and statistical parameters provided in the upper right corner of each panel.

$$OC = 0.634 \times LOI_{550} - 1.83$$

$$IC = Carbonate \times 0.12$$

$$IC = 0.254 \times LOI_{950} - 0.039$$

where OC is organic carbon content (%), IC is inorganic carbon content (%), 0.58 is the Van Bemmelen factor, a commonly used empirical conversion coefficient for estimating the carbon content of organic matter. 0.12 is the relative atomic mass proportion of carbon in calcium carbonate. Since carbonate in lake sediments typically exists in the form of calcium carbonate, this ratio is often used for converting inorganic carbon content. LOI_{550} and LOI_{950} are alternative indicators (%) of organic carbon and inorganic carbon content measured by the loss on ignition method, respectively. The conversion is based on the empirical formula provided by Santisteban et al. (2004).[25] In cases where direct dry bulk density data are unavailable, conversion is performed using the following formula,[26]

$$DBD = 1.776 - 0.363 \times ln(OC \times 10) OC \leq 6\%$$

$$DBD = 1.665 \times (OC) - 0.887 OC > 6\%$$

For records containing only inorganic carbon content data, the DBD is estimated using regional averages from nearby areas. Sedimentation rate data is derived from the depth-age model employing the piecewise linear interpolation method. All chronological data are calibrated to calendar years and corrected for carbon reservoir effects following the original references. Modern lake area and drainage extents are obtained from the HydroSHEDS dataset,[27] which provides global hydrological data at multiple resolutions. The dataset only includes lakes with areas exceeding 0.1 km^2, for smaller lakes, areas are estimated using a Pareto distribution model in this study,[28] yielding a total modern lake area of ~740,000 km^2 in global closed basins.

Model data

The model data used in this study includes outputs from the Paleoclimate Modeling Intercomparison Project (PMIP), the Coupled Model Intercomparison Project Phase 6 (CMIP6) and the Simulation of the Transient Climate of the Last 21000 Years (TraCE-21ka) (Tables S4-S5 & Figure S2). To represent distinct climatic periods, the LGM and MH were selected as millennial-scale cold and warm benchmarks, respectively, while the LIA and MCA were chosen as centennial-scale counterparts. Model selection criteria required the inclusion of at least one paired cold-warm period simulation at the same time scale, ensuring temporal comparability and data source consistency. This approach yielded 11 models from the PMIP3 and 6 models from the PMIP4. All model outputs underwent statistical downscaling with bias correction, and the median values across models at each time scale were used for comparative analysis of different cold and warm periods. For the future projection, 30 models with data for the highest emission scenario (SSP5-8.5) were used for analysis in this study. The TraCE-21ka experiment, recognized as the first fully coupled transient simulation of post-LGM climate evolution, has been extensively applied in studies of climate system evolution patterns and mechanisms.[29-31] Owing to its superior capability in simulating long-term climate continuity since the LGM, this model was employed for continuous lake level simulation in global closed basins.

The climate variables extracted from PMIP and CMIP models comprised monthly precipitation (P) and evapotranspiration (E), while annual P and E data were obtained from the TraCE-21ka model. To analyze the spatiotemporal evolution patterns of lakes in global closed basins since the LGM, we applied Empirical Orthogonal Function (EOF) analysis to the TraCE-21ka simulation outputs. For PMIP/CMIP multi-model ensemble data processing, a statistical downscaling approach incorporating bias correction was implemented.[32] The procedure involved three sequential steps, (1) Bilinear interpolation of individual model outputs to a 0.5° resolution, matching modern observational data; (2) Application of bias correction factors, calculated as the

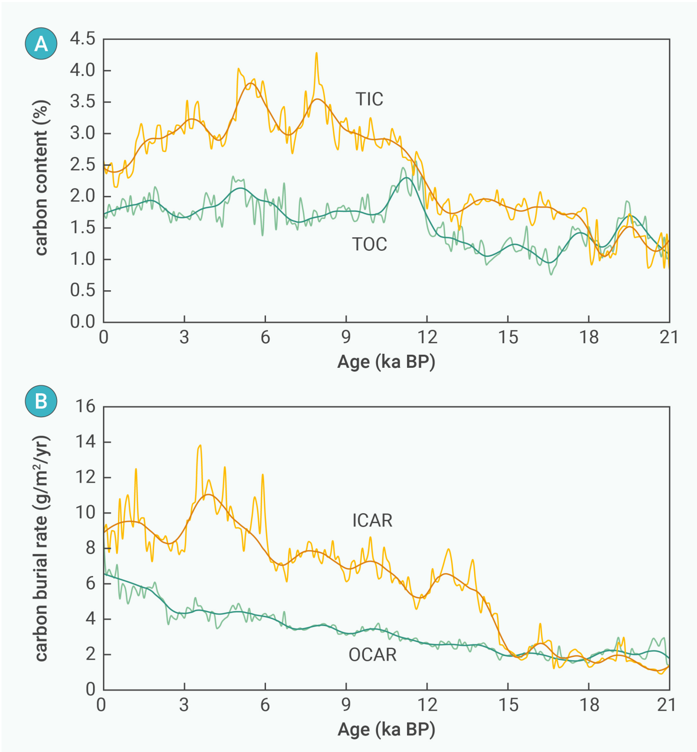

Figure 4. Temporal variations in total organic carbon (TOC) and total inorganic carbon (TIC) content, as well as organic carbon burial rates (OCAR) and inorganic carbon burial rates (ICAR), in lake sediments from global closed basins since the LGM Median values are shown, with smoothed trends generated using the locally weighted scatterplot smoothing (LOWESS) method.

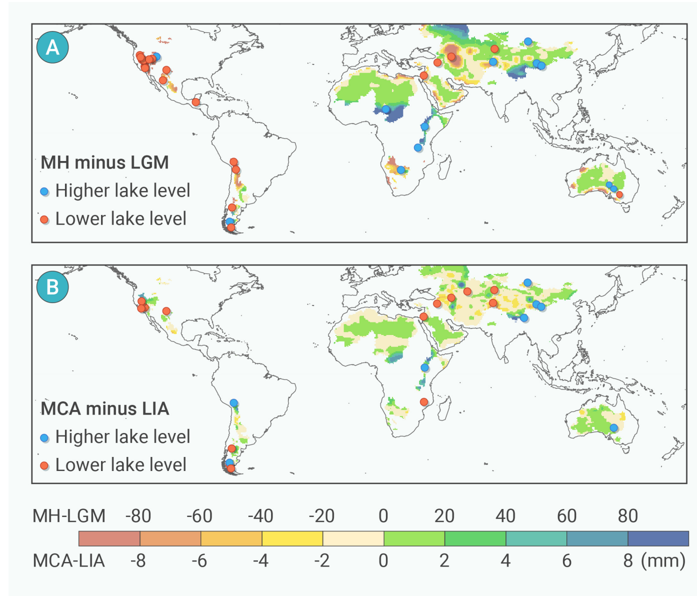

Figure 5. Lake level changes in global closed basins, expressed as differences between the MH and LGM (a) and between the MCA and LIA (b) Blue (red) dots indicate higher (lower) lake levels based on lake level records. Colored grids represent corresponding P-E changes, derived from the median values of the PMIP multi-model ensemble.

ratio of modern observations to model-simulated modern values; (3) Calculation of median values across all models for final analysis. This processing yielded three distinct datasets, (1) Monthly P-E simulations for the LGM, MH, MCA, and LIA periods from PMIP models; (2) Annual P-E projections for 2021-2100 from CMIP models; (3) Centennial-scale P-E reconstructions for 0-21 ka from the TraCE-21ka experiment.

Simulation of lake area change

The water balance in a basin can be expressed by the following formula,[33]

$$\Delta TWS + Q = P - E$$

where ΔTWS represents the change in water storage, Q denotes runoff, P is precipitation, and E is evapotranspiration. In closed basins, there is no external runoff, basin runoff is ultimately reflected in the water volume changes of terminal lakes. When excluding changes in water storage components such as glaciers and groundwater, the formula can be simplified as follows,

$$\Delta V = P - E$$

where ΔV represents the change in lake water volume in closed basins. Assuming constant basin boundaries since the LGM and complete conversion of P-E into lake volume changes, the lake area of closed basins in a specific period can be calculated by the following formula,

$$A_t = \Delta(P - E) \times B \times k + A_0$$

where A_t represents lake area at time t (km^2), $\Delta(P-E)$ is the difference in P-E between time t and modern time (m), B is drainage area (km^2), and A_0 is modern lake area (km^2), k is the conversion coefficient for lake volume-to-area transformation. The relationship between lake water volume and area is typically synchronous and monotonic, with volume increases (decreases) corresponding to area expansions (contractions). The values of k vary significantly across lakes and over time, primarily due to differences in lake basin morphology, introducing substantial uncertainty into lake area calculations at large scales. As an alternative approach, we estimated k as 0.173 based on modern lake volume-area relationships in global closed basins (Figure S3). This P-E based lake area simulation approach has been successfully applied to lakes such as the Caspian Sea[34,35] and represents a robust method for reconstructing lake evolution in data-limited contexts. In this study, the method was applied to simulate past and future lake area changes in global closed basins. Centennial-scale P-E data since the LGM were derived from the TraCE-21ka experiment, while interannual P-E projections for 2021-2100 were obtained from the CMIP6 multi-model ensemble.

RESULTS AND DISCUSSION

Lake carbon burial rate change in global closed basins since the LGM

At the continental scale, organic carbon burial rates in the Asian closed basins during the Holocene are generally lower than those of the African and American closed basins, while inorganic carbon burial rates show the opposite pattern (Figure 2). This spatial variability is likely attributed to regional hydroclimatic conditions. Most African closed basins, located in low-latitude tropical regions under strong influence of the African monsoon, experience high rainfall and vegetation productivity. In contrast, Asian closed basins are predominantly situated in inland regions far from oceanic moisture sources, characterized by arid conditions that favor inorganic carbon accumulation.[8,36] During the Last Deglaciation, continental-scale differentiation in lake carbon burial rates was less pronounced, although inorganic carbon burial rates in Asian closed basins remained consistently high. Temporal analysis of carbon burial rates in global closed basins (Tables S6-S7 & Figure S4) reveals that both organic carbon and inorganic carbon burial rates during the Last Deglaciation are generally lower than those during the Holocene, with an overall increasing trend and greater variability since the LGM.

Based on the Holocene carbon burial rates and modern lake characteristics, we analyzed the responses of lake carbon burial to altitude, temperature, precipitation and lake area (Figure 3). The results indicate that organic carbon burial rates show a significant positive correlation only with temperature, while exhibiting no significant correlation with other factors. In contrast, inorganic carbon burial rates demonstrate a significant positive correlation with altitude and negative correlations with temperature and precipitation, but no significant relationship with lake area. These findings reveal contrasting responses of organic carbon and inorganic carbon burial rates to environmental factors, with inorganic carbon burial appearing more sensitive to climatic and environmental changes than organic carbon burial.

Analysis of integrated sequence changes in lake carbon burial rates of global closed basins since the LGM (Figure 4) reveals distinct temporal patterns. Inorganic carbon content increases prior to 5 ka but declines there-

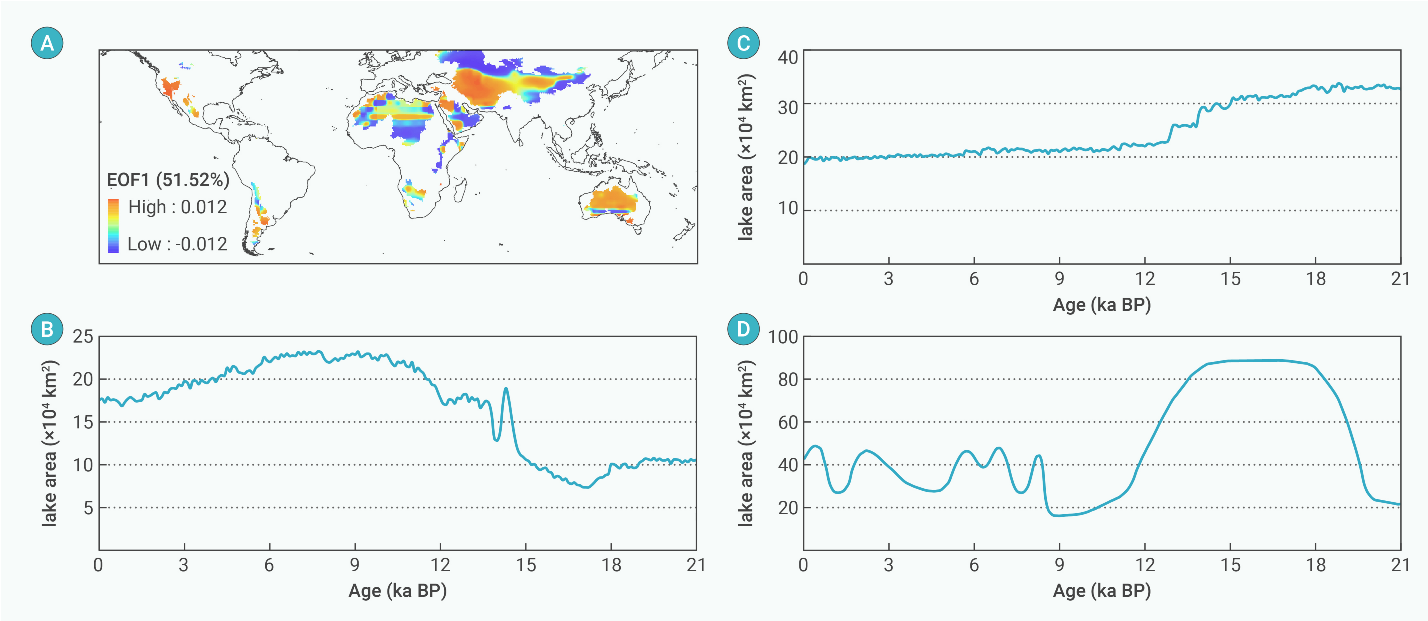

Figure 6. Lake evolution pattern and area calculation results (a) Spatial pattern of the first EOF mode for P-E simulations from the TraCE-21ka model in global closed basins since the LGM, with the variance contribution rate indicated in parentheses. Simulated lake area changes in (b) westerlies-controlled and (c) monsoon-influenced closed basins based on the TraCE-21ka model. (d) Reconstructed lake area changes in the Caspian Sea since the LGM, based on Koriche et al. (2022).

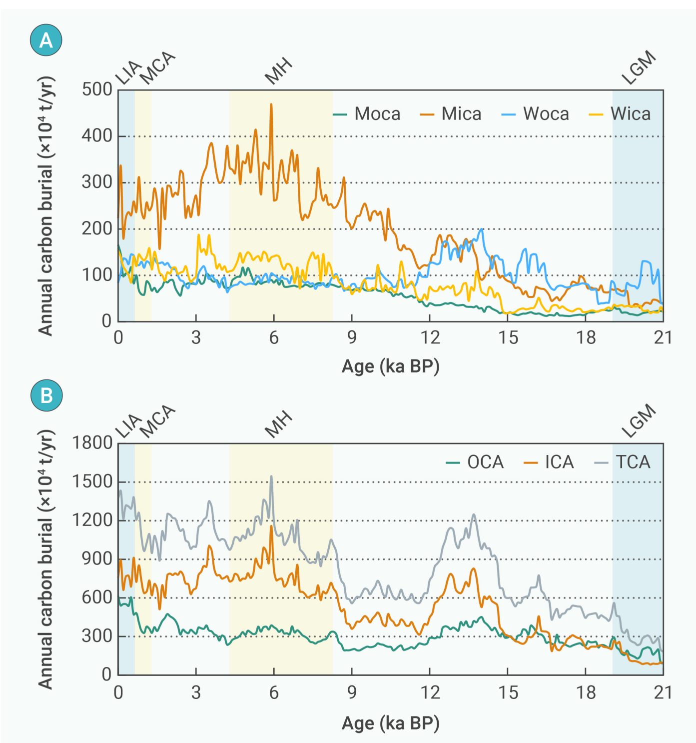

Figure 7. Temporal variations in Lake carbon burial in westerlies-controlled closed basins, monsoon-influenced closed basins and global closed basins since the LGM Moca and Mica denote organic and inorganic carbon burial in monsoon-influenced closed basins, respectively. Woca and Wica represent organic and inorganic carbon burial in westerlies-controlled closed basins, respectively. OCA, ICA and TCA indicate organic, inorganic and total carbon burial in global closed basins, respectively.

after. Notably, organic carbon content exhibits relatively high values between 18 and 21 ka, even exceeding inorganic carbon content during this interval, followed by relatively low values between 5 and 10 ka, when the disparity between organic and inorganic carbon content reaches its maximum. These two periods roughly correspond to the lake expansion during the LGM and lake shrinkage during the MH in the mid-latitude westerlies regions of global closed basins, respectively.[37,38] Carbon burial rates exhibit less complex patterns compared to carbon content variations. Both organic and inorganic carbon burial rates show fluctuating increases since the LGM. After 15 ka, inorganic carbon burial rates increase rapidly, maintaining an upward trend until approximately 3 ka, followed by a phase of overall decline and significant variability. In contrast, organic carbon burial rates increase gradually before 3 ka, with a marked acceleration in recent centuries, despite a concurrent decrease in organic carbon content during the same period. Assuming constant lake areas in global closed basins since the LGM, the total carbon burial is estimated at approximately 147 Pg based on the modern lake area values. The inorganic carbon burial accounts for roughly twice that of organic carbon burial, mirroring the ratio of inorganic carbon to organic carbon in soil carbon pools of global drylands.[8] However, this estimate likely represents a significant underestimation, as it does not account for the presence of larger paleolakes or the substantial carbon preserved in terminal regions of global closed basins.

Lake evolution and area change in global closed basins since the LGM

Lake evolution serves as a critical indicator of hydroclimatic variability, directly reflecting the balance between precipitation and evapotranspiration (precipitation minus evapotranspiration, P-E) within a catchment through changes in lake volume, level and area.[39] Based on lake level records and paleo-hydroclimate model outputs, we compare lake evolution patterns between different cold and warm periods in global closed basins (Figure 5). Results reveal similar spatial distribution at both millennial and centennial scales. Lakes in westerlies-dominated regions, such as the Americas and Central Asia, exhibit higher lake levels during cold periods (LGM and LIA), whereas lakes in monsoon-influenced regions, such as North Africa and East Asia, show higher lake levels during warm periods (MH and MCA). The agreement between lake level records and PMIP P-E simulations reaches 87.5 % and 77.3 % at millennial and centennial scales, respectively, indicating robust model performance in reproducing lake evolution patterns.

However, since PMIP models only provide snapshots for specific periods, we introduce the TraCE-21ka transient climate model to simulate continuous lake area changes over the past 21,000 years, a method validated for lake evolution studies.[34,40] To assess its ability to reproduce the spatial pattern of lake evolution observed in lake level records and PMIP models, we perform an Empirical Orthogonal Function (EOF) analysis on TraCE-21ka P-E simulation data for global closed basins since the LGM (Figure 6). The first EOF mode explains over 50% of the variance and exhibits a spatial pattern consistent with lake level records and PMIP results: positive values in westerlies-dominated regions (e.g., the Americas and Central Asia) and negative values in monsoon-influenced regions (e.g., East Africa and East Asia). Based on

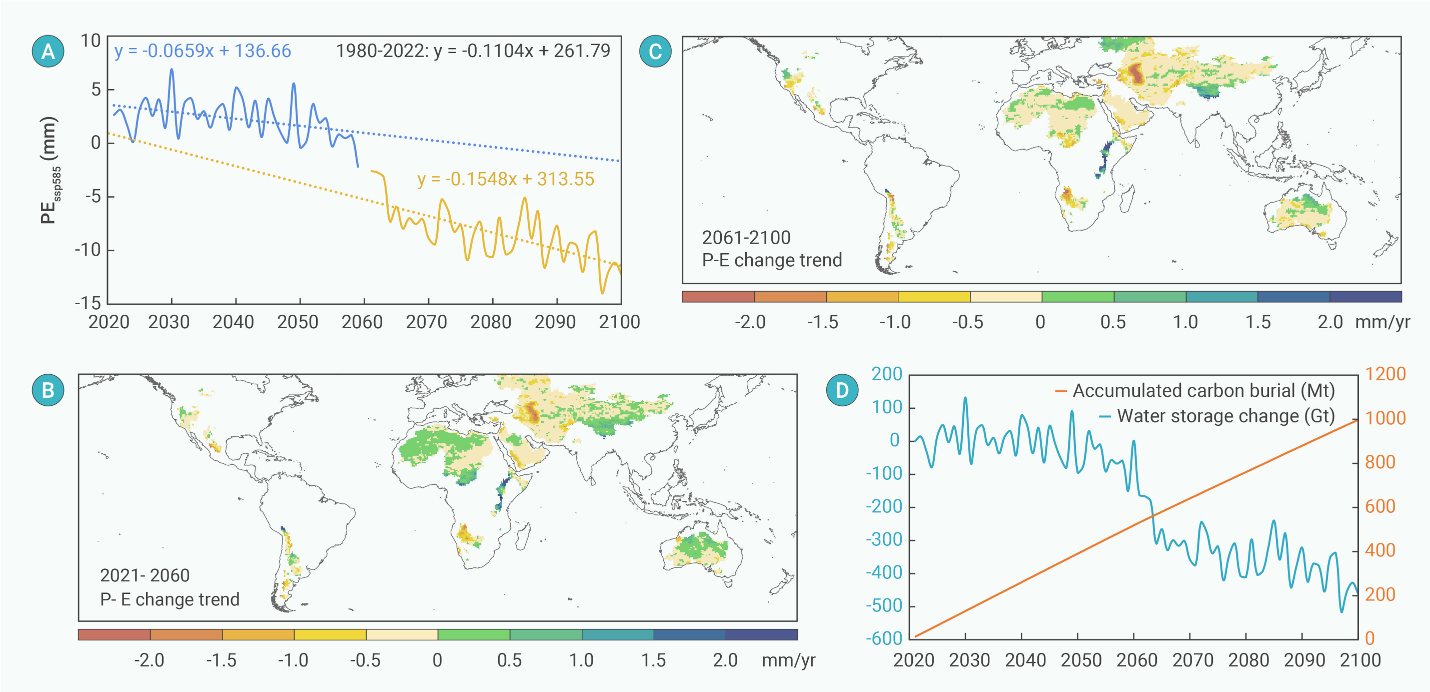

Figure 8. Future hydroclimate and carbon burial changes (A) Projected P-E changes (mm) during 2021-2100 in global closed basins based on CMIP multi-model ensemble. Dotted lines represent linear regression fits, with corresponding equations provided alongside; the black line is based on modern observational data from 1980-2022. Spatial patterns of projected P-E trends (mm/yr) during (B) 2021-2060 and (C) 2061-2100 in global closed basins. (D) Simulated future water storage changes and cumulative carbon burial in global closed-basin lakes from 2021 to 2100.

these EOF results, we classify global closed basins into two categories: westerlies-dominated and monsoon-influenced, each exhibiting distinct lake evolution processes. Lake area changes since the LGM were calculated using an area-weighted average method based on EOF partitioning. The results align well with expectations from lake level records and PMIP multi-model ensembles, except in most Australian and North African (excluding the Chad Basin) closed basins, where positive EOF values contradict previous understanding. To minimize uncertainty, these regions were excluded from further analysis. Additionally, given that the Caspian Sea accounts for approximately half of the total lake area in global closed basins, its area changes since the LGM were calculated separately using water level records from Koriche et al. (2022) to reduce simulation uncertainty.[34] Finally, we obtained the lake area changes in global closed basins since the LGM based on the method of lake area simulation proposed in this study (Figure 6).

Results indicate that the Caspian Sea area reached approximately twice its present size during the Last Deglaciation highstand and decreased to about half its modern extent during the Early Holocene lowstand. These variations fall within a reasonable range, consistent with the observed variability in westerlies- and monsoon-influenced closed basins, where lake areas since the LGM have generally ranged from half to twice their modern sizes. It is important to note that our lake area calculations do not account for meltwater contributions. Fluctuations in land ice sheets and mountain glaciers since the LGM have significantly influenced lake areas, particularly during the rapid warming of the Last Deglaciation, when extensive glacial ablation likely caused substantial regional lake expansion.[41] Consequently, actual lake areas in global closed basins were probably higher than our modeled estimates. Zhang et al. (2018) estimated that the total lake area in China during the MH was approximately 2.5 times larger than modern extents, which is much higher than results from this study.[42] Although direct comparisons are limited by differences in study areas and timescales, this discrepancy suggests that our TraCE-21ka-based simulations likely underestimate lake area changes in global closed basins since the LGM, particularly during the Last Deglaciation and MH periods when high lake levels were prevalent. Therefore, our estimates should be considered a conservative baseline representing the lower limit of plausible lake area changes.

Lake carbon burial in global closed basins since the LGM and its projection

Based on EOF partitioning results, we calculated changes in lake carbon burial rate in westerlies-dominated and monsoon-influenced zones since the LGM. By incorporating lake area changes, we reconstructed carbon burial variations in global closed basins under evolving lake conditions (Figure 7). Organic carbon, inorganic carbon, and total carbon burial exhibit broadly consistent trends, characterized by a fluctuating upward trajectory with distinct phase-specific features. Notable peaks occur during the Bølling–Allerød interstadial (B/A, ~14 ka), MH and the last millennium. The first two peaks correspond to lake expansion under warm and humid conditions in monsoon zones, while the latter likely reflects lake expansion during cold and humid phases in westerlies-dominated regions. Although lakes in the global closed basins were larger during periods of glacial ablation, lower carbon burial rates resulted in total carbon burial not exceeding Holocene levels. In terms of relative contributions to total carbon burial, organic carbon burial in westerlies-dominated zones was more significant during glacial ablation, consistent with increased organic carbon content and lake expansion under cooler and wetter conditions. Conversely, inorganic carbon burial dominated in monsoon-influenced zones during the Holocene, driven by high inorganic carbon burial rates and lake expansion.

Considering lake area changes since the LGM, the total carbon burial in global closed basins is estimated at ~174 Pg, representing a 27 Pg (18%) increase compared to estimates that exclude lake area changes. Of this total, organic carbon burial accounts for ~63 Pg, while inorganic carbon burial contributes ~111 Pg. This ratio closely mirrors the organic-to-inorganic carbon ratio in global dryland soil carbon pools (Plaza et al., 2018). In a broader context, lake carbon burial in global closed basins since the LGM is comparable to China's soil carbon pool (~90 Pg organic carbon and ~60 Pg inorganic carbon),[43] approximately half of global peatland carbon stocks (~410 Pg),[44] one-quarter of the atmospheric carbon pool (~750 Pg) (Houghton, 2007), and one-tenth of the global dryland soil carbon pool.[8]

In recent decades, lakes in global closed basins have experienced progressive desiccation over the past 40 years, with significant shrinkage driven by the combined pressures of climate change and anthropogenic activities.[20,46] This trend has negatively impacted lacustrine carbon burial. Under future global warming scenarios and intensifying human activities, lakes in global closed basins are likely to face even greater challenges. Projecting future changes in these lakes and their carbon burial potential is therefore critical for understanding regional and global water and carbon cycles. Based on CMIP6 SSP585 scenarios for the future, the P-E change in the global closed basins for 2021-2100 was analyzed (Figure 8). The results indicate a continued drying trend, consistent with projected expansions of global drylands.[46] This drying trend occurs in two distinct phases: a moderate phase before 2060 (-0.07 mm/yr), with a slower drying rate compared to the 1980-2022 period (-0.11 mm/yr), followed by an intensified phase after 2060 (-0.15 mm/yr). Spatial analysis of P-E trends reveals that monsoon-influenced closed basins in North Africa, East Africa, East Asia, and northern Australia become wetter by 2060, while most other regions experience drying. This spatial pattern closely resembles dryness-wetness variations observed during millennial- and centennial-scale warm and cold periods, suggesting consistent underlying mechanisms driving past and future hydroclimatic changes in global closed basins. After 2060, the drying trend intensifies and expands across most closed basins, except for those in East Africa and the Tibetan Plateau, which continue to exhibit wetting trends.

Based on simulations of future lake area changes and modern lake carbon burial rates, we projected changes in lake water storage and carbon burial potential in global closed basins from 2021 to 2100 (Figure 8). Under continued future warming, the loss of water storage in global closed basins is projected to reach 500 billion m^3 by 2100, contributing approximately 1.4 mm to global sea level rise. Cumulative carbon burial in closed-basin lakes during this period is estimated at ~1 billion tons, representing a reduction of ~50 million tons compared to scenarios where lake areas remain constant after 2020. These projections highlight the dual pressures facing lakes in global closed basins under future warming: significant water storage loss and reduced carbon sequestration potential. These changes are likely to pose substantial challenges to the ecological integrity and socio-economic development of endorheic river basins in the drylands.

REFERENCES

1. Falkowski P., Scholes R.J., Boyle E., et al. (2000). The Global Carbon Cycle: A Test of Our Knowledge of Earth as a System. *Science* **290**:291–296. DOI:10.1126/science.290.5490.291
2. Archer D. (2010). The Global Carbon Cycle. Princeton University Press. ISBN:9781400837076.
3. McBratney A., Field D.J. and Koch A. (2014). The dimensions of soil security. *Geoderma* **213**:203–213. DOI:10.1016/j.geoderma.2013.08.013
4. Xiang D., Wang G., Tian J., et al. (2023). Global patterns and edaphic-climatic controls of soil carbon decomposition kinetics predicted from incubation experiments. *Nat. Commun.* **14**:2171. DOI:10.1038/s41467-023-37900-3
5. Huang Y.Y., Song X.D., Wang Y.P., et al. (2024). Size, distribution, and vulnerability of the global soil inorganic carbon. *Science* **384**:233–239. DOI:10.1126/science.adi7918
6. Zamanian K., Pustovoytov K. and Kuzyakov Y. (2016). Pedogenic carbonates: Forms and formation processes. *Earth Sci. Rev.* **157**:1–17. DOI:10.1016/j.earscirev.2016.03.003
7. Li Y., Zhang C.Q., Wang N.A., et al. (2017). Substantial inorganic carbon sink in closed drainage basins globally. *Nat. Geosci.* **10**:501–506. DOI:10.1038/NGEO2972
8. Plaza C., Zaccone C., Sawicka K., et al. (2018). Soil resources and element stocks in drylands to face global issues. *Sci. Rep.* **8**:13788. DOI:10.15928/j.1674-3075.202109220332
9. Shen J. (2009). Progress and prospect of palaeolimnology research in China. *J. Lake Sci.* **21**:307–313. DOI:10.18307/2009.0301
10. Guo Y., Zhou Q.H., Wang P., et al. (2023). Research progress on the mechanism of carbon storage in inland waters. *J. Hydroecol.* **44**:141–150. DOI:10.15928/j.1674-3075.202109220332
11. Battin T.J., Luyssaert S., Kaplan L.A., et al. (2009). The boundless carbon cycle. *Nat. Geosci.* **2**:598–600. DOI:10.1038/ngeo618
12. Gao Y., Jia J.J., Lu Y., et al. (2021). Determining dominating control mechanisms of inland water carbon cycling processes and associated gross primary productivity on regional and global scales. *Earth Sci. Rev.* **213**:103497. DOI:10.1016/j.earscirev.2020.103497
13. Du Y.X., Chen F.Z., Zhang Y.L., et al. (2023). Human activity coupled with climate change strengthens the role of lakes as an active pipe of dissolved organic matter. *Earths Future* **11**:e2022EF003412. DOI:10.1029/2022EF003412
14. Zhang F.J., Yao S.C., Xue B., et al. (2017). Organic carbon burial in Chinese lakes over the past 150 years. *Quat. Int.* **438**:94–103. DOI:10.1016/j.quaint.2017.03.047
15. Yang P., Wang N.A., Zhao L.Q., et al. (2021). Variation characteristics and influencing mechanism of CO_2 flux from lakes in the Badain Jaran Desert: A case study of Yindeer Lake. *Ecol. Indic.* **127**:107731. DOI:10.1016/j.ecolind.2021.107731
16. Jia J.J., Sun K., Lü S.D., et al. (2022). Determining whether Qinghai-Tibet Plateau waterbodies have acted like carbon sinks or sources over the past 20 years. *Sci. Bull.* **67**:2345–2357. DOI:10.1016/j.scib.2022.10.023
17. Xiao Q.T., Xu X.F., Qi T.C., et al. (2024). Lakes shifted from a carbon dioxide source to a sink over past two decades in China. *Sci. Bull.* **69**:1857–1861. DOI:10.1016/j.scib.2024.03.022
18. Li Y., Hao L., Han Q., et al. (2022). Provenance of inorganic carbon sinks in closed basins. *Water Resour. Res.* **58**:e2021WR030270. DOI:10.1029/2021WR030270
19. Mendonça R., Müller R.A., Clow D., et al. (2017). Organic carbon burial in global lakes and reservoirs. *Nat. Commun.* **8**:1694. DOI:10.1038/s41467-017-01789-6
20. Wang J.D., Song C.Q., Reager J.T., et al. (2018). Recent global decline in endorheic basin water storages. *Nat. Geosci.* **11**:926–932. DOI:10.1038/s41561-019-0316-8
21. Li Y. and Zhang Y.X. (2020). Synergy of the westerly winds and monsoons in the lake evolution of global closed basins since the Last Glacial Maximum and implications for hydrological change in central Asia. *Clim. Past* **16**:2239–2254. DOI:10.5194/cp-16-2239-2020
22. IPCC. (2013). Climate Change 2013: The Physical Science Basis. Contribution of Working Group I to the Fifth Assessment Report of the Intergovernmental Panel on Climate Change. Cambridge University Press, Cambridge, 1535 pp.
23. Ramsey B.C. (2009). Bayesian analysis of radiocarbon dates. *Radiocarbon* **51**:337–360. DOI:10.1017/S0033822200033865
24. Reimer P.J., Austin W.E.N., Bard E., et al. (2020). The IntCal20 Northern Hemisphere radiocarbon age calibration curve (0–55 cal kBP). *Radiocarbon* **62**:725–757. DOI:10.1017/RDC.2020.41
25. Santisteban J.I., Mediavilla R., López-Pamo E., et al. (2004). Loss on ignition: A qualitative or quantitative method for organic matter and carbonate mineral content in sediments. *J. Paleolimnol.* **32**:287–299. DOI:10.1023/B:JOPL.0000042999.30131.5b
26. Avnimelech Y., Ritvo G., Meijer L.E., et al. (2001). Water content, organic carbon and dry bulk density in flooded sediments. *Aquac. Eng.* **25**:25–33. DOI:10.1016/S0144-8609(01)00068-1
27. Lehner B. and Grill G. (2013). Global River hydrography and network routing: Baseline data and new approaches to study the world's large river systems. *Hydrol. Process.* **27**:2171–2186. DOI:10.1002/hyp.9740
28. Downing J.A., Prairie Y.T., Cole J.J., et al. (2006). The global abundance and size distribution of lakes, ponds, and impoundments. *Limnol. Oceanogr.* **51**:2388–2397. DOI:10.4319/lo.2006.51.5.2388
29. Liu Z., Otto-Bliesner B.L., He F., et al. (2009). Transient simulation of last deglaciation with a new mechanism for Bølling-Allerød warming. *Science* **325**:310–314. DOI:10.1126/science.1171041
30. Cheng J., Liu Z., He F., et al. (2011). Impact of North Atlantic–GIN Sea exchange on deglaciation evolution of the Atlantic meridional overturning circulation. *Clim. Past* **7**:935–940. DOI:10.5194/cp-7-935-2011
31. He F., Shakun J.D., Clark P.U., et al. (2013). Northern Hemisphere forcing of Southern Hemisphere climate during the last deglaciation. *Nature* **494**:81–85. DOI:10.1038/nature11822
32. Tabor K. and Williams J.W. (2010). Globally downscaled climate projections for assessing the conservation impacts of climate change. *Ecol. Appl.* **20**:554–565. DOI:10.1890/09-0173.1
33. Zhang Y.Q., Li C.C., Chiew F.S., et al. (2023). Southern Hemisphere dominates recent decline in global water availability. *Science* **382**:579–584. DOI:10.1126/science.adh0716
34. Koriche S.A., Singarayer J.S., Cloke H.L., et al. (2022). What are the drivers of Caspian Sea level variation during the late Quaternary. *Quat. Sci. Rev.* **283**:107457. DOI:10.1016/j.quascirev.2022.107457
35. Samant R. and Prange M. (2023). Climate-driven 21st century Caspian Sea level decline estimated from CMIP6 projections. *Commun. Earth Environ.* **4**:357. DOI:10.1038/s43247-023-01017-8
36. Ren Z.B., Li C.J., Fu B.J., et al. (2023). Effects of aridification on soil total carbon pools in China's drylands. *Glob. Change Biol.* **30**:e17091. DOI:10.1111/gcb.17091
37. Zhang X.Z., Li Y., Ye W.T., et al. (2020). Wet-dry status change in global closed basins between the mid-Holocene and the Last Glacial Maximum and its implication for future projection. *Clim. Past* **16**:1987–1998. DOI:10.5194/cp-16-1987-2020
38. Li Y. and Zhang Y.X. (2020). Synergy of the westerly winds and monsoons in the lake evolution of global closed basins since the Last Glacial Maximum and implications for hydrological change in central Asia. *Clim. Past* **16**:2239–2254. DOI:10.5194/cp-16-2239-2020
39. Kohfeld K.E. and Harrison S.P. (2000). How well can we simulate past climates. *Evaluating the models using global palaeoenvironmental datasets. Quat. Sci. Rev.* **19**:321–346. DOI:10.1016/S0277-3791(99)00068-2
40. Li Y., Zhang Y., Zhang X., et al. (2020). A continuous simulation of Holocene effective moisture change represented by variability of virtual lake level in East and Central

Asia. *Sci. China Earth Sci.* **63**:1161–1175. DOI:10.1007/s11430-019-9576-x
41. Zhang S., Zhao H., Sheng Y.W., et al. (2022). Mega-lakes in the northwestern Tibetan Plateau formed by melting glaciers during the last deglacial. *Quat. Sci. Rev.* **285**:107528. DOI:10.1016/j.quascirev.2022.107528
42. Zhang F.J., Xue B. and Yao S.C. (2018). The organic carbon storage in Chinese lake sediments during the Holocene Megathermal. *Quat. Sci.* **38**:887-889. Zhang Fengju, Xue Bin, Yao Shuchun. The organic carbon storage in Chinese lake sediments during the Holocene Megathermal[J]. Quaternary Sciences, 2018, 38(4): 887-899. DOI:10.11928/j.issn.1001-7410.2018.04.08.
43. Zheng J.F., Cheng K., Pan G.X., et al. (2011). Perspectives on studies on soil carbon stocks and the carbon sequestration potential of China. *Chin. Sci. Bull.* **56**:2162–2173. DOI:10.1007/s11434-011-4693-7
44. Treat C.C., Kleinen T., Broothaerts N., et al. (2019). Widespread global peatland establishment and persistence over the last 130,000 y. *Proc. Natl. Acad. Sci. U.S.A.* **116**:4822–4827. DOI:10.1073/pnas.1813305116
45. Wurtsbaugh W.A., Miller C., Null S.E., et al. (2017). Decline of the world's saline lakes. *Nat. Geosci.* **10**:816–821. DOI:10.1038/ngeo3052
46. Huang J.P., Yu H.P., Guan X.D., et al. (2016). Accelerated dryland expansion under climate change. *Nat. Clim. Change* **6**:166–171. DOI:10.1038/NCLIMATE2837

FUNDING AND ACKNOWLEDGMENTS

This work was supported by the National Natural Science Foundation of China (42371159). The funders had no role in study design, data collection and analysis, decision to publish, or preparation of the manuscript.

AUTHOR CONTRIBUTIONS

Y. Li conceptualized the study. X. Zhang developed the methodology and conducted the analysis. X. Zhang, Z. Zhang, M. Gao and Y. Xue drafted the manuscript. All authors contributed to the manuscript and approved the final version.

DECLARATION OF INTERESTS

The authors declare no competing interests.

DATA AND CODE AVAILABILITY

Data are available from the corresponding author upon reasonable request

SUPPLEMENTAL INFORMATION

It can be found online at https://doi.org/10.59717/j.xinn-geo.2025.100132